The Cryosphere Discuss., 7, 4065–4099, 2013
www.the-cryosphere-discuss.net/7/4065/2013/
doi:10.5194/tcd-7-4065-2013


The Cryosphere Discussions
Open Access



# Glacier changes in the Karakoram region mapped by multi-mission satellite imagery

**M. Rankl[1], S. Vijay[1], C. Kienholz[2], and M. Braun[1]**

[1]Institute of Geography, University of Erlangen-Nuremberg, Kochstr. 4/4, 91054 Erlangen, Germany
[2]Geophysical Institute, University of Alaska Fairbanks, 903 Koyukuk Drive, Fairbanks, AK 99775-7320, USA

Received: 30 June 2013 – Accepted: 29 July 2013 – Published: 13 August 2013

Correspondence to: M. Rankl (melanie.rankl@fau.de)

Published by Copernicus Publications on behalf of the European Geosciences Union.







## Abstract

Glaciers in the Karakoram region are known to show stable and advancing terminus positions or surging behavior, which contrasts the worldwide retreat of many mountain glaciers. The present study uses Landsat imagery to derive an updated and extended glacier inventory. Surging and advancing glaciers and their annual termini position changes are mapped in addition. Out of 1334 glaciers, 134 show advancing or surging behavior, with a marked increase since 2000. The length distribution of surging glaciers differs significantly from non-surging glaciers. More than 50 % of the advancing/surging glaciers are shorter than 10 km. Besides a regional spatial coverage of ice dynamics, high-resolution SAR data allows to investigate very small and comparably fast flowing glaciers (up to 1.8 m day$^{-1}$). Such data enables mapping of temporal changes of ice dynamics of individual small surging or advancing glaciers. In a further case study, glacier volume changes of three glaciers around Braldu Glacier are quantified during a surge event comparing digital elevation models from the Shuttle Radar Topography Mission (SRTM) and the new TerraSAR-X add-on for Digital Elevation Measurement (TanDEM-X) Mission. We recommend regular acquisitions of high resolution (bi-static) SAR satellite data and further exploitation of the archives in order to generate an improved database for monitoring changes, and to at least partially compensate for the lack of in-situ and long-term climatological measurements in the Karakoram region.

## 1 Introduction

Meltwater from snow cover and glaciers in high mountain areas is a major source for downstream water resources (Church et al., 2011; Immerzeel et al., 2010). Glaciers in the Karakoram and Himalaya contribute to the discharge of the Indus River and its tributaries, which provide water resources and food security for about 200 million people downstream (Immerzeel et al., 2010). The amount of meltwater originating from the mountainous catchment areas is 1.5 times greater than the discharge generated down-





TCD
7, 4065–4099, 2013



stream along the Indus (Immerzeel et al., 2010). Hence, well-founded knowledge of the extent and nature of changes in glaciers supports downstream hydrological planning and water resource management.

Despite the fact that most of the glaciers in the Himalaya are receding (Bolch et al., 2012; Gardelle et al., 2012; Kääb et al., 2012), glaciers in the Karakoram are displaying controversial behavior (Bhambri et al., 2012; Bolch et al., 2012; Gardelle et al., 2012, 2013; Hewitt, 2005; Kääb et al., 2012). Glacier mass balances have been observed to be stable or even positive due to favorable climatic conditions during the last decade (Gardelle et al., 2012; Kääb et al., 2012). Moreover, the Karakoram accounts for a high number of surging glaciers. Glacier surges in the Karakoram have been known since the 1860s (Barrand and Murray, 2006; Copland et al., 2011; Hewitt, 1969, 1998, 2007; Kotlyakov et al., 2008; Mason, 1931), with a marked increase in surge activity in recent years (Copland et al., 2011). Surging glaciers are identifiable by distinctive surface features, such as looped and folded medial moraines, ice foliation, crevassed surfaces, and/or advancing glacier tongues (Barrand and Murray, 2006; Hewitt, 1969; Meier and Post, 1969). During a surge, surface velocities increase by at least one order of magnitude within a few months or up to several years in comparison with non-surging glaciers (Meier and Post, 1969). Moreover, the glacier terminus steepens and thickens throughout a surge event as ice from the reservoir area is shifted to the receiving area (Clarke et al., 1984; Meier and Post, 1969). The rapid advance of the glacier tongue during a surge involves risks of glacial lake outburst floods (GLOFs) by e.g. dammed glacier streams. Thirty-five GLOFs are reported in the Karakoram region since 1826 (Hewitt, 1982; UNDP, 2013).

The present study focusses on the investigation of the temporal and spatial pattern of surging/advancing glaciers across the entire Karakoram Range. Different remote sensing techniques are combined to analyze the highly dynamic behavior of those glaciers. Existing glacier inventories are updated and refined using optical satellite imagery, and a detailed analysis of advancing termini and surges since 1976 is carried out. The inventory is fed with dimensional and topographic characteristics of surging/advancing





TCD
7, 4065–4099, 2013



glaciers, and compared to those of non-surging/normal glaciers. A complete coverage for ice dynamics is achieved from repeat, very high-resolution Synthetic Aperture Radar (SAR) imagery as a composite in the period 2007–2011. High surface velocities close to the glacier snout during a surge event offer further possibilities to identify surging/advancing glaciers. In several case studies, we additionally demonstrate the potential of very high-resolution SAR time series to map changes in ice flow for very small surging/advancing glaciers, and complement this analysis with products based on archived scenes from ERS SAR and ENVISAT ASAR. As a further demonstration in the context of small surging glaciers and new sensor technology, we provide a volume change estimate for two ongoing surges/advances using new bi-static SAR data from the German TerraSAR-X add-on for Digital Elevation Measurement (TanDEM-X) Mission.

## 2 Study site

The Karakoram Range is part of the Hindu–Kush–Karakoram–Himalaya mountain range. It is located between the borders of India, Pakistan, Afghanistan, and China and stretches over ~ 500 km in a NW to SE direction (Fig. 1). The region comprises four peaks higher than 8000 m a.s.l., and half of its surface lies above 5000 m a.s.l. (Copland et al., 2011). The glaciated area covers ~ 17 946 km$^2$ (Bolch et al., 2012) including some of the largest glaciers outside the Polar Regions, e.g., Siachen Glacier (~ 72 km), Baltoro Glacier (~ 64 km), and Biafo Glacier (~ 63 km).

The glaciers in the Karakoram extend over a wide range of elevations (~ 3000 to > 8000 m a.s.l.), while 60 to 80 % of the glaciated area ranges between altitudes of 3800 and 5800 m a.s.l. (Hewitt, 2005). For most glaciers, nourishment is mainly or wholly determined by snow avalanches which also contribute to heavy accumulation of supraglacial debris (Hewitt, 2005). Most of the glaciers flow in steep valleys, and heavily crevassed icefalls are abundant.





TCD
7, 4065–4099, 2013



The climate in the Karakoram is influenced by the Asian monsoons, which contributes to 80 % of the summer precipitation in the southeastern part of the Karakoram Range (Bolch et al., 2012). During winter, precipitation occurs predominantly due to westerly cyclones and is responsible for about two thirds of the snowfall in high altitudes (Bolch et al., 2012). Northward, the steep topography of the Karakoram Range and the more continental location lead to a decreasing influence of both wind systems. Precipitation records are rare for the Karakoram, but Winiger et al. (2005) estimate values of 1600 to 1800 mm $yr^{-1}$ in the southwestern part of the mountain range at altitudes of about 5000 m a.s.l. An increase in winter precipitation in the Karakoram has been observed since the early 1960s (Archer and Fowler, 2004; Bolch et al., 2012; Yao et al., 2012). Moreover, analysis of the ICESat time series from 2003 to 2009 shows a pronounced increase in winter elevation and only a slight summer elevation loss, which implies a slightly increasing mass turnover (Kääb et al., 2012). High altitude meteorological measurements are hardly available for the area of this study. Williams and Ferrigno (2010) found decreasing summer mean and minimum temperatures as well as increasing winter mean and maximum temperatures across the Upper Indus Basin. However, the data used for this analysis originates from stations located at low altitudes of ∼ 1400 to ∼ 2400 m a.s.l. Therefore, it is questionable whether the temperature trend can be applied to the high altitude climate regimes in the Karakoram Range. The positive precipitation trends and the high altitude origins of Karakoram glaciers favored positive surface mass balances of $+0.11 \pm 0.22$ m $yr^{-1}$ water equivalent (w.e.) between 1999 and 2008 for the western part of the Karakoram Range, and $+0.09 \pm 0.32$ m $yr^{-1}$ w.e. between 1999 and 2010 for the eastern part as observed by Gardelle et al. (2012, 2013) by differencing digital elevation models from the respective years. This is confirmed by slightly positive overall elevation changes in the region derived from an ICESat time series from 2003 to 2009 (Kääb et al., 2012).





TCD
7, 4065–4099, 2013



## 3 Data and methods

### 3.1 Glacier inventory and terminus positions

Glacier outlines of surging/advancing glaciers and non-surging/normal glaciers were determined by means of the Randolph Glacier Inventory 2.0 (http://www.glims.org/RGI/randolph.html) as an initial base. These outlines were improved manually in accordance with the guidelines of the Global Land Ice Measurements from Space (GLIMS) (Racoviteanu et al., 2010) in order to use the glacier polygons for a comparison of the characteristics of surging/advancing and non-surging/normal glaciers (e.g., glacier length, area, and slope). We deviated from the GLIMS guidelines when tributary glaciers showed obvious surge/advance behavior and separated them from the main branch. This allowed treating them as individual glaciers in the database. Cloud-free, late summer Landsat scenes from 2009 to 2011, and the SRTM DEM (February 2000) were used to improve the glacier outlines.

We analyzed cloud-free Landsat 1 to 7 imagery (path/row combinations 147/035-036, 148/035-036, 149/034-036, and 150/035, 159/035, and 160/035 for Landsat 1 to 3, Supplement Table 1) to map changes of glacier frontal positions between 1976 and 2012. An annual coverage was available since 1998. Late summer imagery was used and grouped into three categories: prior to 1999, 1999 to 2005, and 2006 to 2012. The advances of glacier tongues could be determined with an accuracy of one to two pixels. We focused the analysis of termini advances on glaciers at least 3 km in length in order to minimize the influence of seasonal snow cover on the derived statistics. In this study, we did not distinguish between surging and advancing glaciers, since a clear identification of surge patterns such as crevassed surfaces was limited with the 30 m resolution of the Landsat imagery. In addition, the temporal scale of the frontal changes did not necessarily allow a separation, because surges can also last several years as shown by Quincey et al. (2011). The number of surging/advancing glaciers was complemented by the observations of Copland et al. (2011). This study





TCD
7, 4065–4099, 2013



compiled an overview on surge events in the Karakoram region, which were identified from literature, by fieldwork or by investigating remotely sensed imagery.

By combining the glacier outlines and the SRTM DEM, we derived a set of parameters which describes the dimensional glacier characteristics. For each glacier, we calculated area and area-altitude distribution (hypsometry), average slope and aspect, and glacier length following the recommendations in Paul et al. (2010). The glacier area parameter was calculated as planar area, i.e., no correction for slope was carried out. The area-altitude distribution was determined in 5 % bins. Calculating the mean of the slopes for the individual grid cells yielded the average glacier slope. The average aspect was obtained by summing the aspect sines and cosines of each cell within a glacier, followed by taking the inverse tangent of the quotient of the two sums. We determined the glacier length by acquiring the length of the longest glacier centerline, which was picked out of a set of centerlines covering the main branches of each individual glacier.

The centerlines were compiled semi-automatically by calculating least-cost routes between glacier heads and termini. The heads (one per glacier branch) were determined by automatically identifying local elevation maxima along the glacier outlines. The termini were set at the lowermost cells along the outlines. Some manual intervention was required if glacier heads were misplaced, or if the automatically derived glacier termini were not at the location of the actual termini. The least-cost route was eventually calculated on a cost-grid individually prepared for each glacier and containing penalty values that decrease toward the glacier center as well as downslope. The resulting least-cost route yielded centerlines that are similar in shape to actual flowlines. The centerlines made possible the accurate determination of glacier length, derivation of average slope and aspect, and measurement of velocity profiles along the centerlines. In a previous study, Barrand and Murray (2006) identified and statistically tested various morphometric factors influencing glacier surges. Based on the new inventory, we provide an update of this statistics using dimensional glacier characteristics, such as glacier length, area, and slope as input parameters for a comparison. The statistical





TCD
7, 4065–4099, 2013



significance of the differences within the specific distributions was tested with a two-sided Wilcoxon rank-sum test (Wilcoxon, 1945).

### 3.2 Glacier surface velocities

Surface velocities were derived using offset intensity tracking on repeat SAR satellite imagery, also known as cross-correlation optimization procedure (Lange et al., 2007; Luckman et al., 2003; Paul et al., 2013; Strozzi et al., 2002). The principle of intensity tracking depends on surface features, e.g., crevasses or large rock boulders, which are detectable in a pair of co-registered images from two different acquisition dates. The displacements of the surface features were tracked on single-look complex images (SLC) using Gamma Remote Sensing Software. The master image was divided into rectangular windows of a given width in range and azimuth (Table 1). For each window the corresponding patch of the slave image was determined based on the normalized cross-correlation between the image patches. When coherence is preserved, the speckle pattern of the two images is correlated. The maximum of the 2-D correlation function located the offsets in range and azimuth direction. Image patches are over-sampled by a factor of 2 to increase the offset estimation accuracy (Werner et al., 2005). The displacement fields were finally geocoded to map coordinates with the SRTM DEM. The technique is well suited to Himalayan-style glaciers due to the presence of respective surface structures (Luckman et al., 2007; Quincey et al., 2011).

Offsets of minor confidence were excluded using a signal-to-noise ratio (SNR) threshold (Table 1). We used TerraSAR-X StripMap (SM) mode single polarization data from 2009 to 2012 and ALOS PALSAR fine beam single polarization (FBS) data from 2007 to 2009 (Supplement Tables 2, 3). While the data takes for the TerraSAR-X imagery may be up to six months apart, most ALOS imagery was acquired with the standard 46 day repeat interval. ERS-1 SAR imagery provided coverage for 1992, 1993, 1998, and 1999 (Supplement Table 4). The complementary ENVISAT ASAR products were used to derive surface velocities for 2003 and 2011 (Supplement Table 4). Pro-





TCD
7, 4065–4099, 2013



cessing for ERS and ENVISAT data was done on 35 day repeat coverage. We used identical settings for the tracking algorithms for all imagery of each sensor (Table 1).

High-resolution SAR imagery makes it possible to map velocities over shorter temporal baselines and for smaller glaciers. Longer wavelengths (e.g., L-band) provide in general more stable backscatter signals over time, thus yielding better results in the structure-less accumulation zone where shorter wavelength imagery tends to decorrelate. Hence, for a best quality velocity product for the entire Karakoram Range we compiled velocity measurements from the various products and sensors, giving priority in subsequent order to the highest resolution, the best SNR and closest acquisition date.

The precision of SAR offset tracking algorithms is dependent on various system, processing, and environmental factors. Those include the temporal and spatial baseline between acquisitions, glacier surface characteristics, and their changes over time as well as spatial representation, spatial resolution, wavelength, temporal changes of surface characteristics, displacements of the glacier in the observation time, tracking window size, step size, search radius, and co-registration accuracy. Those influences are hardly quantifiable and measurable, in particular since they vary from image pair to image pair. However, uncertainties of the specific flow fields can be estimated by determining displacement values over non-moving areas (e.g., bedrock). In order to increase the comparability with other studies, the errors were extrapolated to an annual timescale. Errors for surface movements derived from TerraSAR-X SM and ALOS PALSAR FBS image pairs were $\sim 3$ and $\sim 7\,\mathrm{m\,yr^{-1}}$. ERS-1 SAR and ENVISAT ASAR surface velocities reached errors between $\sim 2.4$ and $\sim 3\,\mathrm{m\,yr^{-1}}$.

### 3.3 Volume changes

In order to estimate the displacement of ice during an ongoing surge/advance, we differenced the SRTM C-band DEM (February 2000) from a newly generated TanDEM-X DEM from 1 January 2012 for Braldu and Skorga Glacier, as well as for an unnamed glacier. The TanDEM-X mission is a recent German bi-static SAR mission, designed





TCD
7, 4065–4099, 2013



to generate a global high-resolution DEM (Krieger et al., 2007). For selected areas, science data takes for DEM generation are made available on request. Details of the two datasets are given in Table 2. The advantage of the quasi bi-static acquisitions of TanDEM-X against conventional repeat pass interferometry is the very limited influence of atmosphere, system noise, and surface motion. We used the Interferometric SAR Processor (ISP) module of Gamma Remote Sensing Software for the InSAR processing of TanDEM-X data (Wegmüller et al., 1998). The TanDEM-X science data consists of two already co-registered SLCs acquired by the tandem constellation of the sensors. We interferometrically processed these SLCs to generate an accurate, high-resolution elevation model. In our case, we used the satellite orbits for flat earth removal. The interferogram was formed using $5 \times 5$ multi-looking in order to preserve a high level of detail and prevent loss of fringes in the high-relief areas. The phase noise, despite very less, in the interferogram was then filtered out by using a Goldstein filter with an exponent value of 0.4 (Goldstein and Werner, 1998). The areas of insufficient coherence ($< 0.3$) were masked out before phase unwrapping. Phase unwrapping was done using a branch-cut algorithm. The baseline refinement and the calibrated absolute phase were supported by fourteen ground control points (GCP) retrieved from the SRTM DEM. For this, the SRTM DEM was converted and resampled back to radar geometry, and the GCPs were extracted over stable rocky areas. The phase, calculated using phase unwrapping, and the absolute heights from SRTM over these points were then simulated using least square estimation technique. The final calibrated product was averaged to 15 m ground resolution as a compromise between reducing noise and loosing detail. The SRTM DEM (C-band, 90 m) is a multiple of this number and thus, facilitated a comparison.

At higher altitudes, significant vertical biases were reported for SRTM (Berthier et al., 2006). We derived the expected error of our elevation product considering two factors: first, the relative error of the TanDEM-X DEM was obtained from a comparison over flat and rocky areas with the SRTM DEM. For this, 82 400 points, summed up to an area of 10 $km^2$, were evaluated and the resulting error was $0.13 \pm 3.27$ m. Second,





TCD
7, 4065–4099, 2013



the C-band penetration into snow and ice over the Central Karakoram is estimated to be ~ 3 to 8 m depending on snow and firn conditions (Gardelle et al., 2012). This corresponded to a mean annual error of ~ 0.25–0.67 m $yr^{-1}$ over the 12 yr period. As X-band also has a certain penetration depth into frozen snow and firn, but less than C-band, we considered this error bar an upper boundary of our uncertainties. Combining both errors, the absolute error for mass change rate was then estimated to 0.60 ± 0.25 m $yr^{-1}$ w.e. using an ice density of 0.9 kg $m^{-3}$.

## 4 Results and discussion

### 4.1 Glacier inventory and terminus positions

The analysis of the Landsat time series across the Karakoram Range revealed that out of about 1334 glaciers, 134 showed termini advances or surged (Fig. 2). Surges and advances can occur in the entire mountain range, but a marked clustering can be observed in the Skamri group, the Sarpo Laggo group, the Panmah group, and in the Upper Shyok River Basin. Glacier surges and advances prior to 1999 occurred mainly in the northwestern part of the Karakoram region, the Sarpo Laggo group and around the Upper Shyok River. These glaciers include the earliest surges (1860s) mentioned in the literature (Copland et al., 2011). The surge of Kichik Khumdan Glacier in the Upper Shyok River Basin between September 1998 and December 1999 was one of the most prominent so far reported. The glacier advanced ~ 975 m (Bhambri et al., 2012) and gained ~ 2.5 $km^2$ in area. Around the Hunza Valley, individual glaciers surged or advanced in this period as well. Between 1999 and 2005, the surging/advancing behavior of the glaciers increased, and a concentration of active behavior was again evident in the central part of the Karakoram, i.e., in the Shakgsgam Valley and the Panmah Glacier Basin (Fig. 2). However, advances and surges can also be observed in several other locations. As Fig. 3 shows, the year 2002 marked the highest number of surging/advancing glaciers with an abrupt decrease in the following year 2003. Fur-





TCD
7, 4065–4099, 2013



ther relative maxima occurred in 2005 and 2010. The extreme values in the temporal pattern of surge/advance events are beyond the first and last quantile, respectively. Further surges/advances might have occurred undetected during the given time interval, since the present study constrained the analysis of optical imagery to advancing termini positions. During the following period, 2006 to 2012, fewer glaciers showed surging/advancing behavior than during the previous period (Fig. 2). By the year 2010, some glaciers had reached the valley bottom or the trunk glacier and had stopped advancing (e.g., glaciers in the Panmah Basin (Fig. 2); Hewitt, 2005), which might partly explain the decreasing number of advancing glaciers since 2010 (Fig. 3). Our results correlate well with observations reported in other studies, such as by Copland et al. (2011) or Hewitt (2005). Heid and Kääb (2012) also provide evidence of surging glaciers in the Karakoram Range from 2000 to 2010 by bi-temporal velocity observations based on Landsat imagery. In many cases, their velocity changes coincide with our analysis of terminus advance or surge. However, there are also glaciers with considerable changes in flow speeds, but no corresponding changes being observed in frontal positions (e.g., Batura or Siachen Glacier, glaciers in the Shimshal Valley). For the peak of surges in 2002, we currently lack a plausible explanation. Unfortunately, limited access to and availability of climate data does not allow a more detailed analysis in this respect.

In a previous study, Barrand and Murray (2006) analyzed potential morphometric and environmental influencing factors on glacier surges, based on 150 glaciers of which 19 were surging. With the inventory of this study we can rely on a much larger database over a longer time period. In our study, the properties of surging/advancing glaciers, i.e., glacier length, area, and slope, were compared with those of non-surging/normal glaciers. The length, area, and slope distributions of surging/advancing and non-surging/normal glaciers (Fig. 4) differed significantly ($p < 0.0001$) referring to a Wilcoxon rang-sum test. The length for surging/advancing glaciers ranged between $\sim 3$ and $\sim 45.5$ km with a median length of 9.3 km. Non-surging/normal glaciers with a length of at least 3 km were considered. The longest glacier was Siachen Glacier





TCD
7, 4065–4099, 2013



with a length of ~ 72 km. The median length of non-surging/normal glaciers was 4.5 km, which might be slightly influenced by the 3 km lower limit of our analysis. Most of the surging/advancing glaciers (> 50 %) were shorter than 10 km (Fig. 4a), which might indicate that short glaciers are more likely to show surging/advancing behavior. This could be a result of shorter reaction times to changing climate conditions, and might be attributed to the observed increased precipitation since the early 1960s (Archer and Fowler, 2004; Williams and Ferrigno, 2010; Yao et al., 2012). The previous study by Barrand and Murray (2006) found a peak in the length distribution of surging glaciers at around 10 km in length. They did not include advancing glaciers. Thus, their observations coincide with our results based on a much larger database.

The distribution of glacier area of non-surging/normal glaciers shows the highest percentages between 2 to 10 $km^2$ with a peak at around 3 $km^2$, while surging/advancing glaciers have a maximum percentage of around 10 $km^2$ (Fig. 4b). The histogram of the area distribution of surging/advancing glaciers seems to be shifted toward larger areas.

The histogram of the distribution of the average slope of the glacier surface shows (Fig. 4c) that surging/advancing glaciers mainly range between 15° and 25°, with a median of 18°. Non-surging/normal glaciers seem to extend over slightly steeper slopes. The mean minimum elevation of surging/advancing glaciers is 4410 m a.s.l., and the mean maximum elevation is 6361 m a.s.l. Non-surging/normal glaciers range between 4672 m a.s.l. and 5967 m a.s.l. The analysis indicates that surging/advancing glaciers cover a wider range of elevations than non-surging/normal glaciers in the Karakoram region. Thus, no direct relation of surge-/advance-type with elevation or slope could be established.

### 4.2 Glacier surface velocities

Surface velocity maps were derived from TerraSAR-X SM, ALOS PALSAR FBS, ERS-1 SAR and ENVISAT ASAR image pairs for the years, 1992, 1993, 2003, and 2006 to 2012. Figure 5 provides the best velocity coverage (2007 to 2011) of the Karakoram Range derived from different sensors with priority given to the highest resolution and





TCD
7, 4065–4099, 2013



best coverage for each individual glacier. Large swath sensors like ERS and ENVISAT provide high spatial coverage at one time interval, however, exclude displacements of small glaciers. The latter are best resolved with TerraSAR-X imagery, but lead to a combination of different time steps. Although the suitability of such a composite velocity map is limited for glaciers with temporally highly variable ice flow, it provides an overview of the entire region with maximum spatial detail, and is of relevance for many other glaciers showing no such highly dynamic behaviors. The velocity fields of very large glaciers, such as Batura, Hispar, Biafo, Chogo Lungma, Baltoro or Siachen Glacier can be well identified. Notably, Hispar Glacier has the lowest surface velocities of all the very large glaciers, with speeds decreasing close to zero already at the lowest third of the glacier. The general flow pattern is as to be expected for mountain glaciers with highest velocities in the central or upper part of the glacier close to the equilibrium line altitude. However, various smaller glaciers show high flow speeds closer to the terminus, e.g., Yazghil Glacier flowing north into the Shimshal Valley. This glacier drains from a rather wide high-altitude catchment into a narrow, channel-like valley, leading to channelized flow. Pronounced high surface velocities can also be observed close to the terminus at various glaciers, where ongoing advances and surges have been previously reported or are shown in this study (such as with Tatulu Gou Glacier, Quincey et al., 2011). The potential of high-resolution SAR to map short-term changes in ice flow is demonstrated subsequently.

At the Panmah Basin, southwest of the Shakgsam Valley, eight glaciers showed advancing or surging behavior in the past (Hewitt, 2005; Copland et al., 2011). Four of them (Drenmang, Chiring, Maedan, Shingchukpi Glaciers, Fig. 6a) advanced during the last two decades and have been classified as surge-type glaciers (Hewitt, 2005). The Landsat image analysis showed that these tributaries have reached the main trunk of the Nobande Sobonde Glacier and stopped advancing by 2008 or 2010. South of these tributaries, the northwest flowing 1st Feriole Glacier showed termini advances. The glacier started advancing in 2002 (Fig. 6b). By March 2012, it had advanced ~ 2.0 km (Fig. 6b). Flow fields derived from TerraSAR-X SM image pairs for a 22 day





TCD
7, 4065–4099, 2013



interval between December 2009 and January 2010 indicated high surface velocities of $\sim 1.25\,\mathrm{m\,day^{-1}}$ near the glacier's snout (Fig. 6d). In March 2011, surface velocities increased up to $\sim 1.78\,\mathrm{m\,day^{-1}}$ and again slightly decrease in June 2013 (Fig. 6c and d). The shape of the center line surface velocity profiles indicates the advance of 1st Feriole Glacier and the propagation of the surge front towards the glacier's terminus. The advancing tongue, the crevassed glacier surface, and high surface velocities close to the snout clearly identify 1st Feriole Glacier as a surge-type glacier. However, the recent decrease in surface velocities might indicate the decay of the active surge-phase.

In the Shaksgam Valley, including the Skamri and Sarpo Laggo Basin, we found a high number of surging/advancing glaciers (Fig. 7). The potential of the high-resolution TerraSAR-X imagery to map ice dynamics of very narrow glaciers also becomes obvious from catchments #68, #77, #82, #93, #95, #102, #113 or #119 (Fig. 7a). The comparably high flow speeds throughout the glaciers or at the terminus indicate an active phase of a surge or advance. This corresponds neatly with the mapped frontal position changes (Fig. 7b). Quincey et al. (2011) previously showed a similar pattern of high flow velocities at the surge front of Kunyang Glacier (a tributary of Hispar Glacier). A good example of a small surging/advancing glacier is Musita Glacier (#67), which revealed high surface velocities of $\sim 0.5\,\mathrm{m\,day^{-1}}$ (June to September 2009) close to its snout. The analysis of the optical imagery indicated a frontal advance of $\sim 0.85\,\mathrm{km}$ from 2005 to 2009.

Centerline velocity profiles (Fig. 8) showed the changes in surface flow over time for selected surging/advancing and non-surging/normal glaciers (the location of those glaciers is marked in Fig. 1). Skamri Glacier (#122 in Fig. 7b) was identified by Copland et al. (2009) as a surge-type glacier. The surge happened prior to 1973 (Copland et al., 2009). South Skamri Glacier that surged in 1990 (#80 in Fig. 7b) showed active behavior in 2007 (Copland et al., 2009, 2011), and still in 2009 (Fig. 8a). Since 1990, South Skamri Glacier represented the dominant glacier in the Skamri Basin, pushing Skamri Glacier's tongue aside. The tracking results for 1992 (Fig. 8b) are consistent for Skamri Glacier at comparably high values of up to $0.8\,\mathrm{m\,day^{-1}}$. These high values might





TCD
7, 4065–4099, 2013



still be attributed to an active phase or its decay. Surface velocities for Skamri Glacier decreased between 2003 and 2009 (up to 0.3 m day$^{-1}$), which supports the fact, that South Skamri Glacier was the dominant flow unit in the Skamri Basin at that time (Copland et al., 2009). However, during 2011, Skamri Glacier accelerated considerably to ~ 1.5 m day$^{-1}$. Flow velocities for South Skamri Glacier decreased slightly from 2009 to 2011. The comparison of the centerline velocity profiles between these two glaciers may indicate that after the South Skamri Glacier had represented the dominant ice-flow unit since the early 1990s, Skamri Glacier showed active behavior in 2011, and might influence South Skamri Glacier again in the following years, as was the case prior to 1990.

Batura Glacier (~ 58 km) is one of the longest glaciers in the Karakoram region (Bishop et al., 1995) and the largest west of the Hunza Valley. The glacier originates at an altitude of ~ 6200 m on the north-facing slopes of the Batura Mustagh (7795 m) and flows in a WE direction, terminating in the Hunza Valley at 2516 m. Five main ice units and more than 20 tributaries compose the glacier system. The Karakoram Highway crosses its meltwater stream and follows the terminal moraine for about 2 km. Therefore, knowledge about the state of the glacier is important due to its proximity to vulnerable infrastructure. Precipitation in the upper accumulation area is about 1000 to 1300 mm yr$^{-1}$, which is ten times higher than in the Hunza Valley (BGIG, 1979, 1980). High amounts of avalanches contribute to the glacier's mass and to the heavily debris-covered glacier tongue (Edwards, 1960; Finsterwalder, 1960; Shi, 1984). Batura Glacier is characterized as a non-surging glacier (BGIG, 1979; Bishop et al., 1995). However, the glacier terminus approached the Hunza Valley between the 19th century and the middle of the 1940s. In 1973/74, the glacier meltwater stream destroyed a major bridge and parts of the Karakoram Highway embankment in the Hunza Valley (UNDP, 2013). The Batura Glacier Investigations Group (BGIG) (1979) predicted frontal advances for the 1980s and threatening of the downslope Karakoram Highway. However, the predicted advance never occurred. Instead, the glacier showed frontal retreat and downwasting of the glacier surface (Bishop et al., 1995; Williams and Fer-





TCD
7, 4065–4099, 2013



rigno, 2010). Data on surface velocities of Batura Glacier are rare. Bishop et al. (1995) mentioned ice velocities of 517.5 m yr$^{-1}$ below an ice fall and 0.3 m yr$^{-1}$ near the terminus. However, the exact location of the measurements is unknown. The BGIG (1979) reported averaged velocities of $\sim$ 100 m yr$^{-1}$ across the tongue in the mid-1970s. Ice velocities increase toward the firn line and decrease toward the terminus, which is also visible in Fig. 5. The longitudinal centerline velocity profiles (Fig. 8c) are measured on the northern tributary, which merges with the southern flow unit about 20 km from the terminus. Between kilometer 10 and 20, surface velocities show an increase for 2006, 2007, and 2009. This part of the profile represents the area where the northern and southern flow units merge. The longitudinal profile for May to June 2006 shows increased surface velocities, which might be due to the speed-up of surface flow during summer months (Bishop et al., 1995; Copland et al., 2009). Williams and Ferrigno (2010) suggest that Batura Glacier has undergone ice flow stagnation since the middle of the 1940's. However, Batura Glacier shows considerable inter-annual fluctuations of surface velocities between 1992 and 2011 as this analysis shows (Fig. 8c).

### 4.3 Volume changes

Besides an improved knowledge of terminus position and ice flow, the change in ice volume over time is another important variable. For Braldu and Skorga Glacier, we demonstrate the potential of TanDEM-X bi-static SAR acquisitions to determine volume and mass changes due to surging/advancing glaciers. Figure 9 shows the elevation change based on a difference between the SRTM C-band DEM from February 2000 and an interferometric TanDEM-X DEM from 1 January 2012. Braldu Glacier reveals a distinct pattern of considerable surface lowering at the central lower part of the glacier (up to 100 m in 12 yr), while almost no lowering is observed at the glacier snout. The ice velocity map (Fig. 5) shows almost no movement at the tongue, and the inspection of the optical imagery reveals that this area is heavily debris-covered and hence, providing substantial protection against ablation. On the other hand, the marked flow pattern in the lowering zone originates from movement of the looped moraines, and possibly





TCD
7, 4065–4099, 2013



different melt amounts between bare ice and heavily debris-covered strips. In the accumulation area of Braldu Glacier almost no changes are observed. Only limited mass gain seems to have occurred at the easternmost tributary. Remarkable, however, is the pronounced thickening of Skorga Glacier and glacier #1 at their snouts. The analysis of the Landsat imagery also showed termini advances since 1998/99. While the elevation in the immediate termini area increased by almost 100 m in the twelve-year period from February 2000 to January 2012, a larger area just above showed less pronounced lowering, and higher catchment areas a slight gain in elevation. These patterns nicely show, how the surge moved down-glacier, and how the glacier is recovering in the highest areas. Integrating the elevation changes over the entire catchment revealed a mass change rate of $+2.98 \pm 1.87\,\mathrm{m\,yr^{-1}}$ w.e. over the twelve year period (applying an ice density of $0.9\,\mathrm{kg\,m^{-3}}$) for glacier #1 and $+2.96 \pm 2.52\,\mathrm{m\,yr^{-1}}$ w.e. for Skorga Glacier. Other studies calculated comparable glacier elevation changes derived from differencing the SRTM DEM (February 2000) and a DEM computed from SPOT5 imagery (December 2008) (Gardelle et al., 2012), and from the analysis of ICESat time series from 2003 to 2008 (Kääb et al., 2012). Gardelle et al. (2012) classified Braldu Glacier as a surge-type glacier that surged before 2000. The present study found no evidence that Braldu Glacier had surged or advanced since 1976 from the analysis of Landsat imagery. However, the observed elevation change pattern is in agreement with the classification by Gardelle et al. (2012). Thus, we suggest that the surge of Braldu Glacier occurred prior to 1976.

## 5 Conclusions and outlook

The present study utilized different remote sensing based methods to generate an updated glacier inventory of the Karakoram region. It provides a new comprehensive dataset on surging/advancing glaciers in the Karakoram region, including the temporal and spatial evolution of glacier front positions. The analysis revealed that 134 out of 1334 glaciers were surging/advancing glaciers. We were able to show tempo-





TCD
7, 4065–4099, 2013



ral changes in the surge/advance behavior, which is expressed in an increase in the number of surging/advancing glaciers since 2000, with a maximum in 2002. A statistical significant difference in glacier length distribution of surging/advancing glaciers and non-surging/normal glaciers could be identified. The surge and advance pattern could be linked to changes in ice dynamics as observed from multi-temporal and multi-resolution SAR imagery. The high spatial and temporal resolution of especially X-band SAR imagery proofed highly suitable to monitor ice-flow dynamics of small and comparably fast-flowing glaciers (e.g., on-going surges). Geometric distortions in the SAR imagery due to the side-looking sensor system and the steep, mountainous terrain could be avoided by choosing proper orbit and path settings. The potential of the new bi-static TanDEM-X Mission to accurately quantify the displacement of ice during a surge/advance could be demonstrated in an example. Based on this extended datasets, findings of previous studies could be confirmed and extended in regard to the number and location as well as timing of glacier surges or advances. However, from a glaciological point of view, it remains unclear, which external factors drive the surge/advance behavior in the Karakoram. Unfortunately, no reliable climate data was available to link the observations to changes in surface mass balance or possible meteorological triggering events or years. Reports by other authors have indicated slight mass gains from several years up to decades due to stronger westerlies. The high number of small surging/advancing glaciers detected in this study supports such a hypothesis due to the general shorter response times of small glaciers.

Our results demonstrate the high potential modern high-resolution SAR missions have for deriving surface velocity fields, including those for small and comparably fast-flowing valley glaciers during surge events. Short repeat cycles of eleven or 22 days enable the identification of surface structures with only a limited temporal decorrelation impact. The study on ice dynamics also confirmed that X-band with its shorter wavelength, does decorrelate rapidly in the structure-less accumulation zone of the Karakoram, where longer wavelengths (e.g., from L-band ALOS PALSAR) still preserve the signal over 46 days. It is recommended that at least annual repeat acquisitions with





TCD
7, 4065–4099, 2013



short temporal baselines should be integrated into the acquisition plans of current and future SAR missions for regions with highly dynamic and fast changing glaciers such as the Karakoram Range. The exploitation of the satellite archives (e.g., ERS, ENVISAT, Landsat) provides additional potential for determining changes in flow patterns and surge cycles, which is important for monitoring glaciers in remote and inaccessible regions such as the Karakoram Range.

The data from the TanDEM-X mission analyzed here, demonstrates that elevation and mass changes can be mapped very accurately using data from the new bi-static SAR mission. It provides a weather-independent tool in addition to the photogrammetric and laser-altimetry missions, with the main advantage of providing coherence and elevation information in the bright and texture-less accumulation areas. The high spatial resolution is a further asset to study mountain glaciers, while issues of penetration depth under different snow and meteorological conditions are limiting factors. Those effects need to be studied in more detail in order to provide accurate error estimates for the derived change products.

**Supplementary material related to this article is available online at http://www.the-cryosphere-discuss.net/7/4065/2013/tcd-7-4065-2013-supplement.pdf.**

*Acknowledgements.* This study was kindly supported with TerraSAR-X and TanDEM-X data under DLR AOs LAN_0164 and mabra_XTI_GLAC0264. ENVISAT ASAR and ERS-1/2 SAR imagery were accessed under ESA AO 3575. USGS kindly granted access to the Landsat image archive. The authors were financially supported by the University of Erlangen-Nuremberg, DFG grant BR2105/8-1 in the “Schwerpunktprogramm Antarktisforschung” as well as by the HGF Alliance “Remote Sensing of Earth System Dynamics”.





TCD
7, 4065–4099, 2013



## References


Archer, D. R. and Fowler, H. J.: Spatial and temporal variations in precipitation in the Upper Indus Basin, global teleconnections and hydrological implications, Hydrol. Earth Syst. Sci., 8, 47–61, doi:10.5194/hess-8-47-2004, 2004.

Barrand, N. and Murray, T.: Multivariate controls on the incidence of glacier surging in the Karakoram Himalaya, Arct. Antarct. Alp. Res., 38, 489–498, 2006.

Batura Glacier Investigations Group (BGIG): The Batura Glacier in the Karakoram Mountains and its variations, Sci. Sin., 22, 958–974, 1979.

Batura Glacier Investigations Group (BGIG): Karakoram Batura Glacier, Exploration and Research, Academia Sinica, Science Press, Beijing, 1980.

Berthier, E., Arnaud, Y., Vincent, C., and Remy, F.: Biases of SRTM in high-mountain areas: implications for the monitoring of glacier volume changes, Geophys. Res. Lett., 33, L08502, doi:10.1029/2006GL025862, 2006.

Bhambri, R., Bolch, T., Kawishwar, P., Dobhal, D. P., Srivastava, D., and Pratap, B.: Heterogeneity in Glacier response from 1973 to 2011 in the Shyok valley, Karakoram, India, The Cryosphere Discuss., 6, 3049–3078, doi:10.5194/tcd-6-3049-2012, 2012.

Bishop, M. P., Shroder Jr., J. F., and Ward, J. L.: SPOT multispectral analysis for producing supraglacial debris-load estimates for Batura glacier, Pakistan, Remote Sens. Images Tech. Notes, 10, 81–90, 1995.

Bolch, T., Kulkarni, A., Kääb, A., Huggel, C., Paul, F., Cogley, J. G., Frey, H., Kargel, J. S., Fujita, K., and Scheel, M.: The state and fate of Himalayan glaciers, Science, 336, 310–314, 2012.

Church, J. A., White, N. J., Konikow, L. F., Domingues, C. M., Cogley, J. Graham, Rignot, E., Gregory, J. M., van den Broeke, Michiel R, Monaghan, A. J., and Velicogna, I.: Revisiting the Earth's sea-level and energy budgets from 1961 to 2008, Geophys. Res. Lett., 38, L18601, doi:10.1029/2011GL048794, 2011.

Clarke, G., Collins, S., and Thompson, D.: Flow, thermal structure, and subglacial conditions of a surge-type glacier, Can. J. Earth Sci., 21, 232–240, 1984.

Copland, L., Pope, S., Bishop, M., Shroder, J., Clendon, P., Bush, A., Kamp, U., Seong, Y., and Owen, L.: Glacier velocities across the central Karakoram, Ann. Glaciol., 50, 41–49, 2009.






TCD
7, 4065–4099, 2013



Copland, L., Sylvestre, T., Bishop, M., Shroder, J., Seong, Y., Owen, L., Bush, A., and Kamp, U.: Expanded and recently increased glacier surging in the Karakoram, Arct. Antarct. Alp. Res., 43, 503–516, 2011.
de Lange, R., Luckman, A., and Murray, T.: Improvement of satellite radar feature tracking for ice velocity derivation by spatial frequency filtering, IEEE T. Geosci. Remote, 45, 2309–2318, 2007.
Edwards, J. I.: The Batura Muztagh Expedition, 1959, Alpine J., 65, 48–52, 1960.
Finsterwalder, R.: German glaciological and geological expeditions to the Batura Mustagh and Rakaposhi Range, J. Glaciol., 3, 787–788, 1960.
Gardelle, J., Berthier, E., and Arnaud, Y.: Slight mass gain of Karakoram glaciers in the early twenty-first century, Nat. Geosci., 5, 322–325, 2012.
Gardelle, J., Berthier, E., Arnaud, Y., and Kääb, A.: Region-wide glacier mass balances over the Pamir-Karakoram-Himalaya during 1999–2011, The Cryosphere Discuss., 7, 975–1028, doi:10.5194/tcd-7-975-2013, 2013.
Goldstein, R. M. and Werner, C. L.: Radar interferogram filtering for geophysical applications, Geophys. Res. Lett., 25, 4035–4038, doi:10.1029/1998GL900033, 1998.
Heid, T. and Kääb, A.: Repeat optical satellite images reveal widespread and long term decrease in land-terminating glacier speeds, The Cryosphere, 6, 467–478, doi:10.5194/tc-6-467-2012, 2012.
Hewitt, K.: Glacier surges in the Karakoram Himalaya (central Asia), Can. J. Earth Sci., 6, 1009–1018, 1969.
Hewitt, K.: Natural dams and outburst floods of the Karakoram Himalaya, IAHS, 138, 259–269, 1982.
Hewitt, K.: Recent Glacier Surges in the Karakoram Himalaya, South Central Asia, available at: www.agu.org/eos_elec/97016e.htm, American Geophysical Union, 1998.
Hewitt, K.: The Karakoram anomaly? Glacier expansion and the "elevation effect," Karakoram Himalaya, Mountain Res. Develop., 25, 332–340, 2005.
Hewitt, K.: Tributary glacier surges: an exceptional concentration at Panmah Glacier, Karakoram Himalaya, J. Glaciol., 53, 181–188, 2007.
Immerzeel, W. W., van Beek, L. P. H., and Bierkens, M. F. P.: Climate change will affect the Asian water towers, Science, 328, 1382–1385, 2010.





TCD
7, 4065–4099, 2013



Kääb, A., Berthier, E., Nuth, C., Gardelle, J., and Arnaud, Y.: Contrasting patterns of early twenty-first-century glacier mass change in the Himalayas, Nature, 488, 495–498, doi:10.1038/nature11324, 2012.

Kotlyakov, V. M., Osipova, G. B., and Tsvetkov, D. G.: Monitoring surging glaciers of the Pamirs, central Asia, from space, Ann. Glaciol., 48, 125–134, 2008.

Krieger, G., Moreira, A., Fiedler, H., Hajnsek, I., Werner, M., Younis, M., and Zink, M.: TanDEM-X: A satellite formation for high-resolution SAR interferometry, IEEE T. Geosci. Remote, 45, 3317–3341, 2007.

Luckman, A., Murray, T., Jiskoot, H., Pritchard, H., and Strozzi, T.: ERS SAR feature-tracking measurement of outlet glacier velocities on a regional scale in East Greenland, Ann. Glaciol., 36, 129–134, 2003.

Luckman, A., Quincey, D., and Bevan, S.: The potential of satellite radar interferometry and feature tracking for monitoring flow rates of Himalayan glaciers, Remote Sens. Environ., 111, 172–181, 2007.

Mason, K.: Expedition notes: tours of the Gilgit Agency, Himalayan J., 3, 110–115, 1931.

Meier, M. F. and Post, A.: What are glacier surges?, Can. J. Earth Sci., 6, 807–817, doi:10.1139/e69-081, 1960.

Paul, F., Barry, R. G., Cogley, J. G., Frey, H., Haeberli, W., Ohmura, A., Ommanney, C. S. L., Raup, B., Rivera, A., and Zemp, M.: Recommendations for the compilation of glacier inventory data from digital sources, Ann. Glaciol., 50, 119–126, 2010.

Paul, F., Bolch, T., Kääb, A., Nagler, T., Nuth, C., Scharrer, K., Shepherd, A., Strozzi, T., Ticconi, F., Bhambri, R., Berthier, E., Bevan, S., Gourmelen, N., Heid, T., Jeong, S., Kunz, M., Lauknes, T., Luckman, A., Merryman, J., Moholdt, G., Muir, A., Neelmeijer, J., Rankl, M., VanLooy, J., and van Niel, T.: The Glaciers Climate Change Initiative: methods for creating glacier area, elevation change and velocity products, Remote Sens. Environ., Climate Change Initiative Special Issue, accepted, 2013.

Quincey, D. J., Braun, M., Glasser, N. F., Bishop, M. P., Hewitt, K., and Luckman, A.: Karakoram glacier surge dynamics, Geophys. Res. Lett., 38, L18504, doi:10.1029/2011GL049004, 2011.

Racoviteanu, A. E., Paul, F., Raup, B., Khalsa, S. J. S., and Armstrong, R.: Challenges and recommendations in mapping of glacier parameters from space: results of the 2008 Global Land Ice Measurements from Space (GLIMS) workshop, Boulder, Colorado, USA, Ann. Glaciol., 50, 53–69, 2010.





TCD
7, 4065–4099, 2013



Shi, Y.: Some studies of the Batura glacier in the Karakoram Mountains, in: The International Karakoram Project, 1, Cambridge University Press, Cambridge, 51–63, 1984.
Strozzi, T., Luckman, A., Murray, T., Wegmüller, U., and Werner, C.: Glacier motion estimation using SAR offset-tracking procedures, IEEE T. Geosci. Remote, 40, 2384–2391, 2002.
UNDP: Bureau for Crisis Prevention and Recovery: Glacial lake outburst floods, available at: http://www.managingclimaterisk.org/project-countries.html, 2013.
Wegmüller, U., Werner, C., and Strozzi, T.: SAR interferometric and differential interferometric processing chain, Geoscience and Remote Sensing Symposium Proceedings, IGARSS '98, 1106–1108, 1998.
Werner, C., Wegmüller, U., Strozzi, T., and Wiesmann, A.: Precision estimation of local offsets between pairs of SAR SLCs and detected SAR images, Proceedings of IGARSS '05, 2005.
Wilcoxon, F.: Individual comparisons by ranking methods, Biom. Bull., 1, 80–83, 1945.
Williams, R. J. and Ferrigno, J.: Glaciers of Asia: US Geological Survey Professional Paper 1386-F, United States Government Printing Office, Washington, 2010.
Winiger, M., Gumpert, M., and Yamout, H.: Karakorum–Hindukush–western Himalaya: assessing high-altitude water resources, Hydrol. Process., 19, 2329–2338, 2005.
Yao, T., Thompson, L., Yang, W., Yu, W., Gao, Y., Guo, X., Yang, X., Duan, K., Zhao, H., Xu, B., Pu, J., Lu, A., Xiang, Y., Kattel, D. B., and Joswiak, D.: Different glacier status with atmospheric circulations in Tibetan Plateau and surroundings, Nat. Clim. Change, 2, 663–667, doi:10.1038/nclimate1580, 2012.





TCD
7, 4065–4099, 2013



**Table 1.** Overview of sensors and main characteristics used for velocity mapping. The parameter setting for feature tracking like tracking window size, step size and SNR threshold for discarding unreliable measurements is also listed per sensor.

| Sensor | Sensor wavelength, platform repeat cycle | Tracking window size (range × azimuth) | Step (range/ azimuth) | SNR threshold |
|---|---|---|---|---|
| ALOS PALSAR FBS | 23.5 cm, L-band, 46 days | 64 × 192 | 12/36 | > 7 |
| TerraSAR-X SM | 3.1 cm, X-band, 11 days | 128 × 128 | 25/25 | > 7 |
| ERS-1 SAR | 5.6 cm, C-band, 35 days | 64 × 320 | 6/30 | > 5 |
| ENVISAT ASAR | 5.6 cm, C-band, 35 days | 64 × 320 | 6/30 | > 5 |





TCD
7, 4065–4099, 2013



**Table 2.** Characteristics of the two digital elevation models used for volume change estimates.

| Data | Band | Wavelength | Date | Effective baseline/ height of ambiguity | Spatial resolution |
|---|---|---|---|---|---|
| SRTM DEM | C band | 5.6 cm | 22 Feb 2000 | 60 m | 90 m |
| TanDEM-X DEM | X band | 3.1 cm | 1 Jan 2012 | 103 m/73.8 m | Processed to 15 m |





TCD
7, 4065–4099, 2013



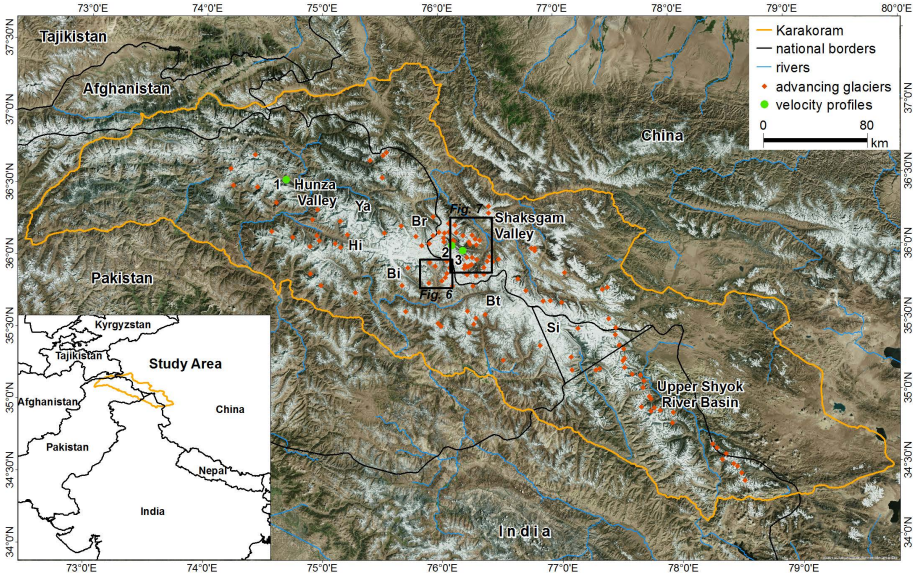


**Fig. 1.** Overview map of the Karakoram Range. The orange line indicates the delineation of the study region. Known advances of glaciers are indicated with red dots. The locations of major glaciers and groups are indicated (abbreviations denote: Ba = Batura Glacier, Bi = Biafo Glacier, Br = Braldu Glacier, Bt = Baltoro Glacier, Hi = Hispar Glacier, Si = Siachen Glacier, Ya = Yazghil Glacier). Green dots mark glaciers with velocity profiles shown in the results section (1 = Batura Glacier, 2 = Skamri Glacier, 3 = South Skamri Glacier). Locations of Figs. 6 and 7 are outlined.





TCD
7, 4065–4099, 2013



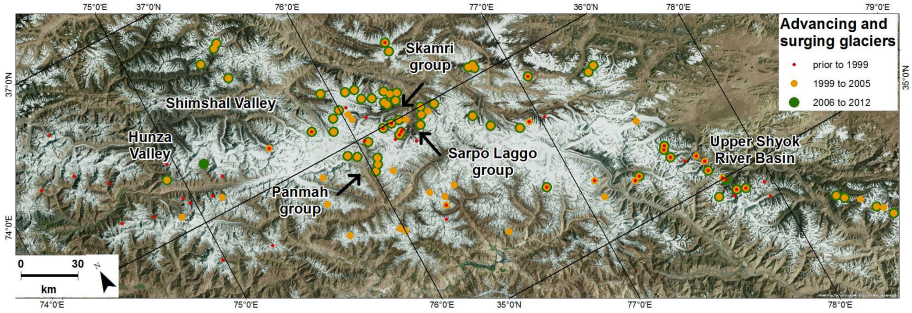


**Fig. 2.** Distribution of surging/advancing glaciers across the Karakoram Range. Surges in the different periods (prior to 1999, 1999 to 2005, and 2006 to 2012) are marked in different colors.





TCD
7, 4065–4099, 2013



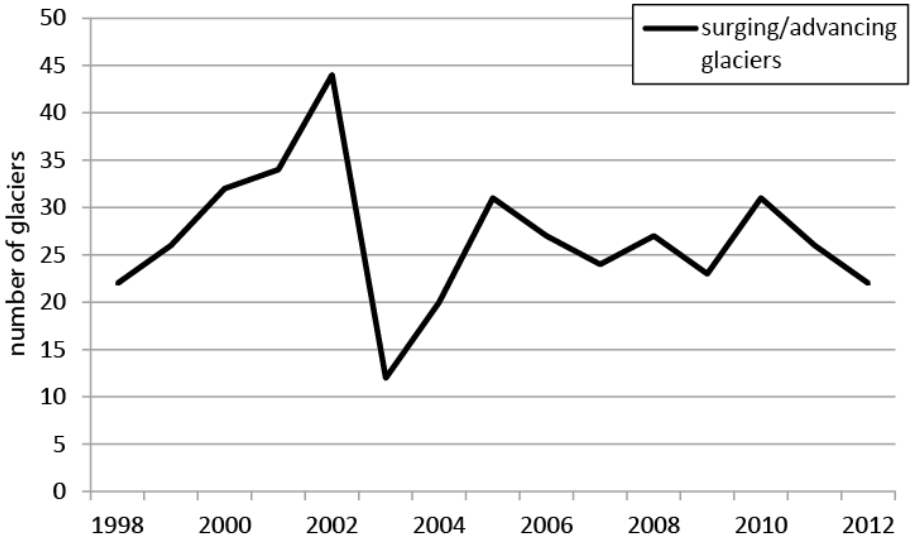


**Fig. 3.** Temporal course of surging/advancing glaciers between 1998 and 2012. A peak in 2002 followed by a marked decrease in 2003 can be observed.





TCD
7, 4065–4099, 2013



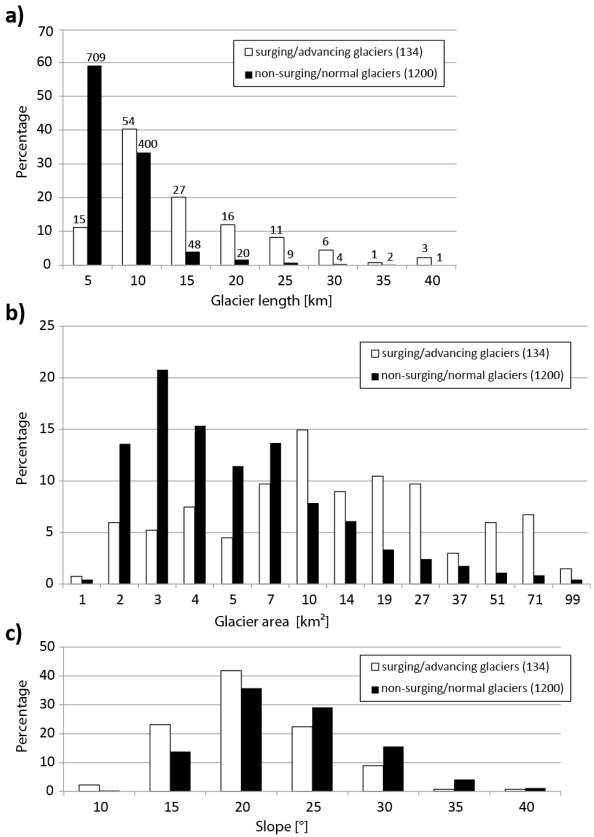


**Fig. 4.** Percentages of surging/advancing and non-surging/normal glaciers related to the overall number of surging/advancing and non-surging/normal glaciers, divided into classes of **(a)** glacier lengths, **(b)** catchment area and **(c)** mean slope. The absolute numbers per glacier length class are given above the bar in **(a)**.





TCD
7, 4065–4099, 2013



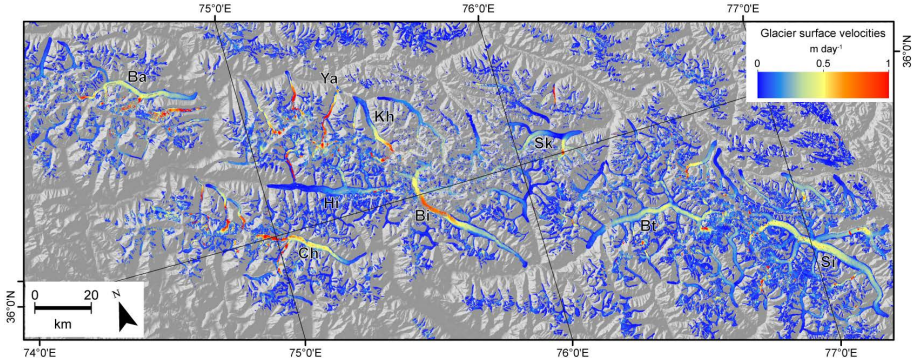


**Fig. 5.** Compiled surface velocities mosaic of the Karakoram Range. Priority has been given to the highest resolution and best coverage. Data takes are between 2007 and 2011 from TerraSAR-X, ALOS PALSAR and ENVISAT ASAR. Abbreviations denote: Ba = Batura Glacier, Bi = Biafo Glacier, Bt = Baltoro Glacier, Ch = Chogo Lungma Glacier, Hi = Hispar Glacier, Kh = Khurdopin Glacier, Si = Siachen Glacier, Sk = Skamri Glacier, Ya = Yazghil Glacier.





TCD
7, 4065–4099, 2013



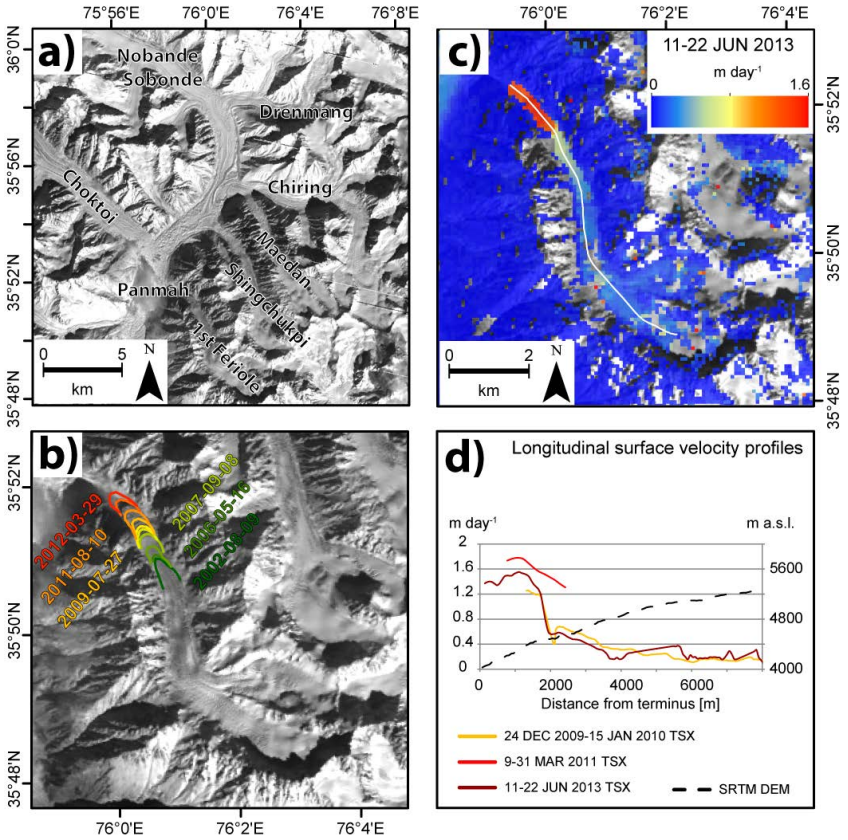


**Fig. 6.** Termini advances and surface velocities for 1st Feriole Glacier, Panmah Basin **(a)**. **(b)** shows the changing terminus positions since 2002. A surface velocity map derived from repeat TerraSAR-X SM imagery between 11 and 22 June 2013 is given in **(c)**, and **(d)** comprises the centerline velocity profiles and their changes over time (location of the profiles is marked in **(c)**).





TCD
7, 4065–4099, 2013



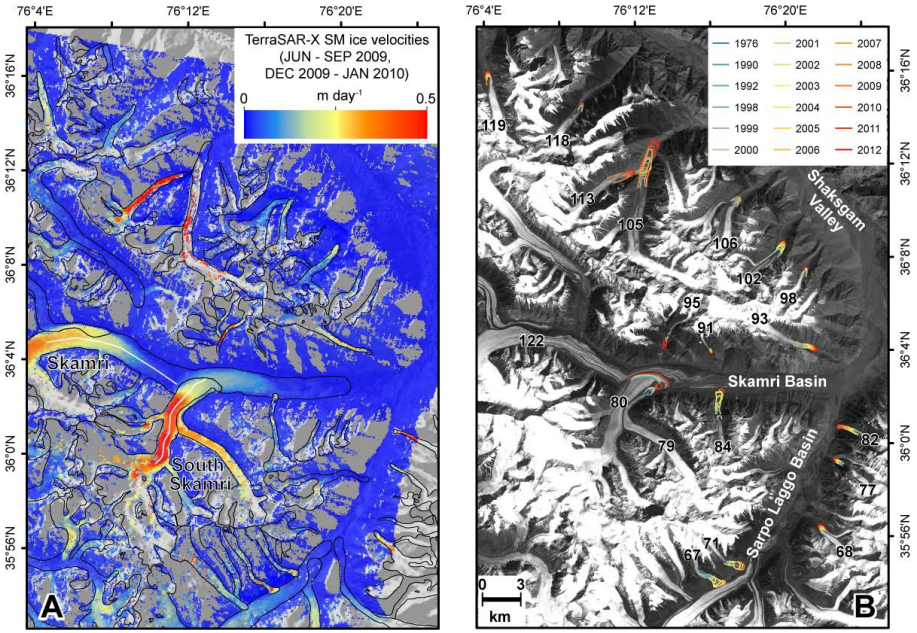


**Fig. 7.** Surface velocities **(A)** derived from TerraSAR-X SM image pairs (16 June 2009 to 12 September 2009 and 24 December 2009 to 15 January 2010) and glacier surges/advances **(B)** in the Sarpo Laggo, Skamri Basin, and central Shaksgam Valley.





TCD
7, 4065–4099, 2013



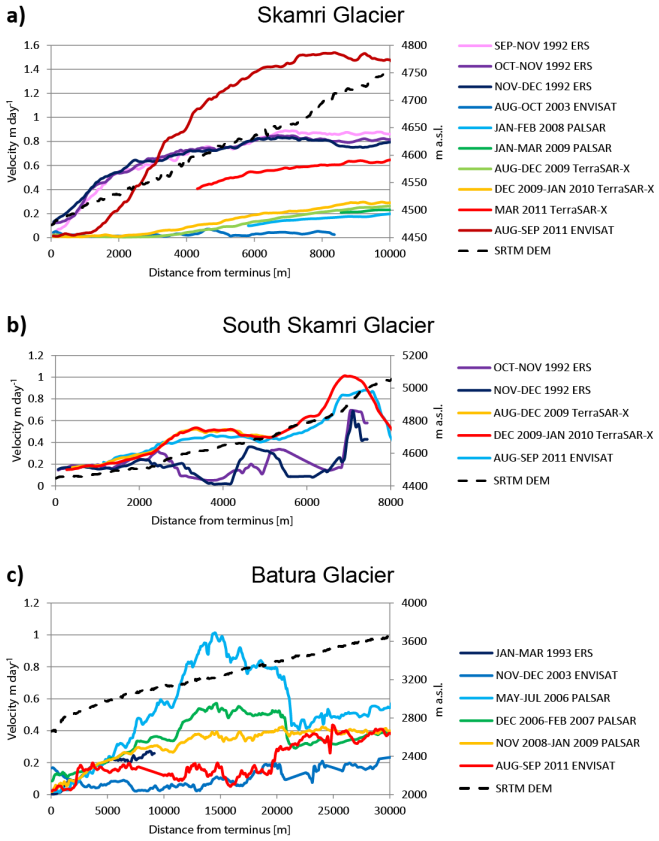


**Fig. 8.** Velocity profiles along the centerline of Skamri **(a)**, South Skamri **(b)**, and Batura Glacier **(c)**.





TCD
7, 4065–4099, 2013



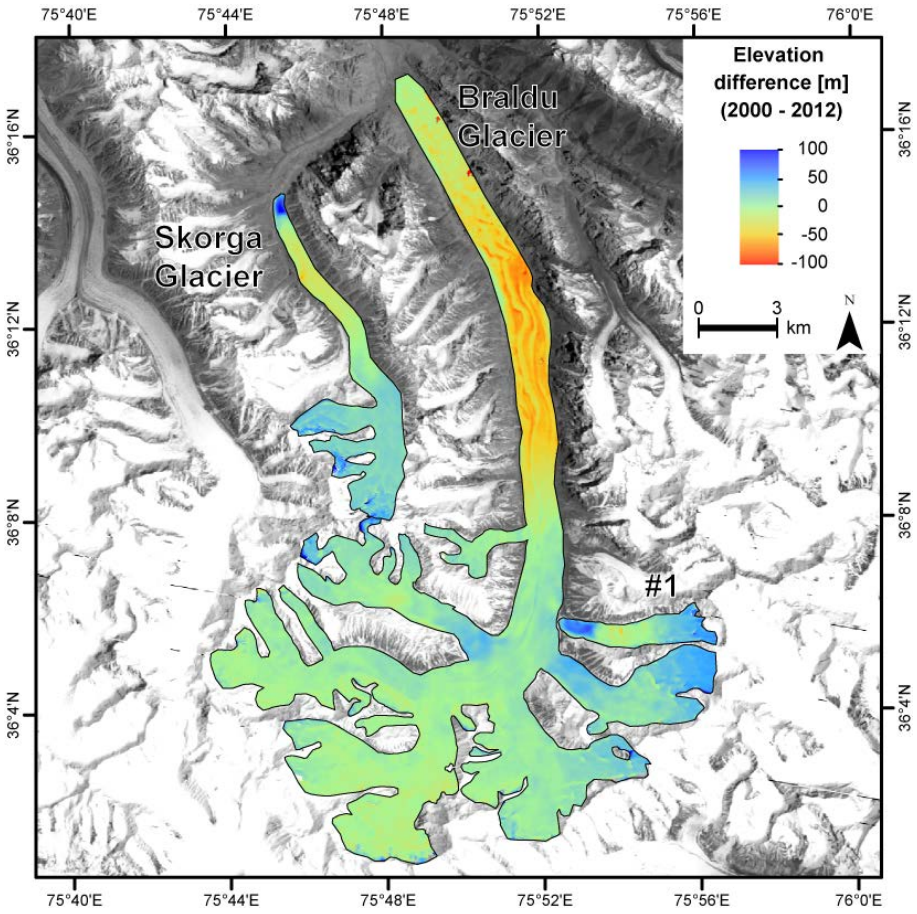


**Fig. 9.** Elevation changes between SRTM (February 2000) and TanDEM-X (1 January 2012) for Braldu, Skorga, and an unnamed glacier.





TCD
7, 4065–4099, 2013